Bulletin of Electrical Engineering and Informatics
Vol. 13, No. 3, June 2024, pp. 2165~2174
ISSN: 2302-9285, DOI: 10.11591/eei.v13i3.7122

Nonlinear control of three level NPC inverter used in PV/grid system: comparison of topologies and control methods

Youness Atifi, Abdelhadi Raihani, Mohammed Kissaoui, Rachid Lajouad, Khalid Errakkas
Electrical Engineering and Intelligent Systems Laboratory (EEIS), ENSET Mohammedia, Hassan II University of Casablanca, Casablanca, Morocco

Article Info

Article history:

Received Jul 2, 2023
Revised Nov 27, 2023
Accepted Mar 30, 2024

Keywords:

Control
Integral backstepping
Neutral point clamped inverter
Proportional integral controller
Smart grid

ABSTRACT

With the passage of time, the importance of using renewable energy systems to overcome energy consumption and improve the quality of the grid has emerged through the use of nonlinear control techniques and reliance on advanced types of inverters such as multi-level inverters. This research is focused on comparing two grid-connected converter topologies in a photovoltaic (PV) generation system connected to a three-phase grid that serves a non-linear load. Additionally, the study explores two different control techniques applied to this converter, evaluating their effects on the total harmonic distortion coefficient. A comparison has been made between the traditional inverter and the three-level inverter type neutral point clamped (NPC) inverter, with the use of integral backstepping (IBS) technique which was also compared with the proportional integral (PI) controller. The simulation results in MATLAB/Simulink are presented illustrating the performances and the strong effectiveness of the three-level NPC inverter controlled by the proposed technique (IBS).

Corresponding Author:

Youness Atifi
Electrical Engineering and Intelligent Systems Laboratory (EEIS), ENSET Mohammedia
Hassan II University of Casablanca
Casablanca, Morocco
Email: atifi.youness@gmail.com

1. INTRODUCTION

In recent years, the consumption of electrical energy has grown very strongly, and it seems that this consumption will continue to increase given several parameters, such as economic growth and the rise in per capita electricity consumption. To face this reality and to keep pace with life, it is necessary to think of distributed production systems instead of centralized production. This production is based on renewable energy generators; photovoltaic (PV) generators are part of these distributed sources [1]-[7]. PV cells contribute to reducing reliance on fossil fuels and mitigating the emission of harmful pollutants into the environment. Furthermore, the use of PV cells enhances the quality of life for individuals residing in areas without electricity. PVs are economical in the long run, as they reduce energy costs and increase the energy efficiency of the systems that use them [8]-[11]. In addition, PV systems can now be used to improve the quality of electrical energy, such as through the dissolution of current load harmonics and the compensation of reactive load power [7].

Solar panels are usually connected to a controlled converter in order to track the maximum power point. Different methods can be used, such as the perturb and observe method or the increased conductivity method, and different techniques are relied upon to implement them, such as traditional methods, fuzzy logic, or artificial neural networks [12]-[16]. On the other hand, a grid-side converter can be used to regulate the

exchange of energy between a PV system and the electrical power grid, allowing for the production of electrical power that meets quality standards [17], [18]. In situations where nonlinear loads are extensively utilized within power systems, the emergence of harmonic currents and reactive power flow in the supply lines becomes more pronounced. As a result, effective control of the grid-side converter is essential to maintaining control over the mutual power exchange between the PV system and the grid, thereby ensuring the high quality of the energy produced by the PV system.

Generally, in the literature, we note that the work deals with the control of simple two-level inverters, and even those treated by multilevel inverters have been limited to the classic maximum power point tracking (MPPT) control of the chopper that is upstream of the inverter. It is also noted that there is little work done by nonlinear control of multilevel neutral point clamped (NPC) inverters, or that the work is limited to conducting simulations or carrying out experiments for one type of inverter without comparisons or testing of parameter changes. A PV generation system connected to the grid via an inverter controlled by the back-stepping technique was studied and simulated with the regulation of the DC link voltage by the sliding mode technique [7]. During the research, no comparison was made with another technology or even with an inverter of another type. Sliding mode control-support vector machine (SMC-SVM) technology was used to control the NPC-type inverter within the grid-connected PV power generation system, and the results showed the effectiveness of the proposed system, but the results were not compared to other technology, and more importantly, the system was not tested for non-linear loads [17]. A multi-objective control strategy was developed to improve system performance based on non-linear control methods [19]. The proposed system controls both the turbine and the PV panels to track the maximum power area, and it also contributes to regulating the DC link voltage and reactive power compensation. The researchers focused on the MPPT control unit and correcting the power factor without giving importance to the used inverter, which was of the traditional type. The focus was on improving the performance of a three-level NPC inverter and overcoming the limitations imposed by traditional linear control methods by proposing a unique method to design the inverter weighting factors based on an artificial neural network (ANN) [20]. The results and the proposed mechanism show important data, but the system has not been tested when there are non-linear loads or when the inverter is used to connect the PV panels to the grid.

This work will mainly focus on controlling the grid-side inverter in order to reduce the harmonic distortion content. The research aims to compare the performance of a traditional bridge converter and a three-level NPC converter used in a PV generation system connected to a nonlinear electrical network. The research will also provide a comparison between the performance of integrated back-end controllers, as one of the non-linear control techniques, and proportional integral (PI) controllers in regulating ac grid currents and reducing the value of the total harmonic distortion coefficient of the currents passing into the electrical grid. During the research, PQ theory was used to determine harmonic currents. This paper is organized as follows: the study of PV/grid interconnection stages (system description) is dealt with in section 2. In section 3, the design of the grid-side converter (GSC) control system using backstepping techniques and PQ theory, which were used to determine the harmonic currents, was explained. Section 4 is reserved for simulation results and concludes with section 5, which concludes the work.

2. SYSTEM DESCRIPTION

In this research, the system with the notations of Table 1 shown in Figure 1 is studied, which consists of: i) PV panels, ii) DC-DC boost converter, iii) NPC inverter connected to the grid through a link filter, and iv) non-linear load.

2.1. DC-DC converter

DC-DC converter is the first stage from PV/grid interfacing system, where the inverter is the second one. The DC-DC converter must be controlled to extract the maximum power available from PV panels. The model of the DC-DC converter which is boost converter adopted in this paper is shown in Figure 2, its dynamic model is given in (1)-(3) [21], [22]. For designing MPPT control unit in this paper, perturb and observe (P&O) algorithm was used, which its flowchart is which was mentioned in [13], where D is the duty cycle.

$$\frac{V_o}{V_s} = \frac{1}{1-D} \tag{1}$$

$$\frac{dI_s}{dt} = \frac{-(1-D)V_o+V_s}{L} \tag{2}$$

$$\frac{dV_o}{dt} = \frac{(1-D)I_s-I_o}{C} \tag{3}$$

Table 1. List of notations

Notation	Designation	Notation	Designation
$V_{a-grid}, V_{b-grid}, V_{c-grid}$	Power grid voltages	V_{dc}	DC bus voltage
V_d, V_q	Power grid voltages in d-q coordinates	V_{dc_1}, V_{dc_2}	DC capacitor voltages
$V_{\alpha-grid}, V_{\beta-grid}$	Power grid voltages in α-β coordinates	R_{filter}	Decoupling filter resistor
i_{ga}, i_{gb}, i_{gc}	Power grid currents	L_{filter}	Decoupling filter inductance
$v_{a-filter}, v_{b-filter}, v_{c-filter}$	NPC voltages	C_{NPC}	NPC capacitor
$u_{dfilter}, u_{qfilter}$	NPC voltages in d-q coordinates	V_g	RMS grid voltage
$i_{NPC\_(a,b,c)}$	NPC currents	F_g	Power grid frequency
$i_{dfilter}, i_{qfilter}$	NPC currents in d-q coordinates	R_{Load}	Nonlinear load resistor
$i_{a-Load}, i_{b-Load}, i_{c-Load}$	Nonlinear load currents	L_{Load}	Nonlinear load inductance
$i_{\alpha-Load}, i_{\beta-Load}$	Load currents in α-β coordinates		

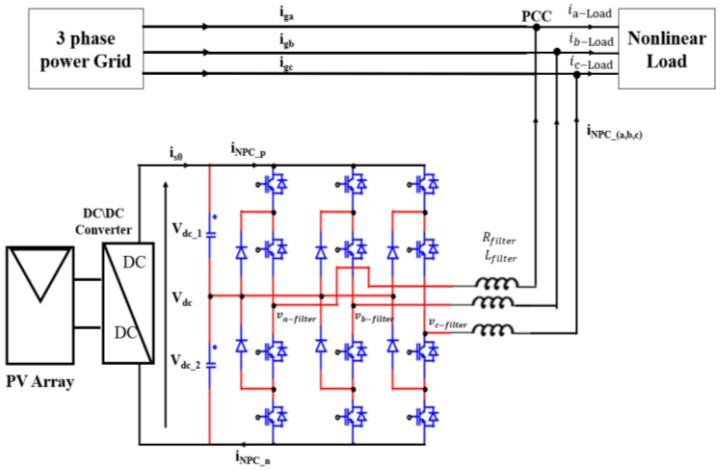

Figure 1. Structure of an electrical PV/grid system

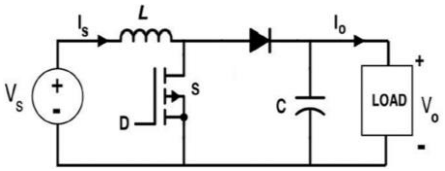

Figure 2. The structure of the boost chopper

2.2. Neutral point clamped inverter

In the multilevel inverters, there are several structures, namely the H-bridge cascade structure, the floating capacitor structure, and finally the structure adopted in this work, which was shown in Figure 1, has a neutral point very recognized by the NPC structure. The advantage of this structure compared to other structures is that it requires fewer capacitors and fewer power switches to generate the desired voltage levels at the output. It can be added that this NPC structure is very effective in power supply systems. The control of the NPC inverter must meet certain constraints in order to ensure the proper functioning of the PV system and improve the quality of electric power [7], [17], [20].

3. CONTROL SYSTEM DESIGN OF GRID SIDE CONVERTER

Figure 3 shows the block diagram of the whole system. It consists of two control loops: the external regulation loop, in which the DC link voltage is regulated using a PI regulator, and the internal regulation loop, in which the alternating currents exchanged with the grid are regulated. Here, backstepping techniques were used, and its performance was compared with that of PI controllers through the effect of its performance on the value of the total harmonic distortion coefficient. In the power stage, a comparison was presented between the traditional inverter and the NPC multi-level inverter in terms of their effect on the deformation coefficient. It should be noted that the reference values of the currents exchanged with the grid are computed in the α−β frame, where the method of its conclusion is explained in the following paragraph.

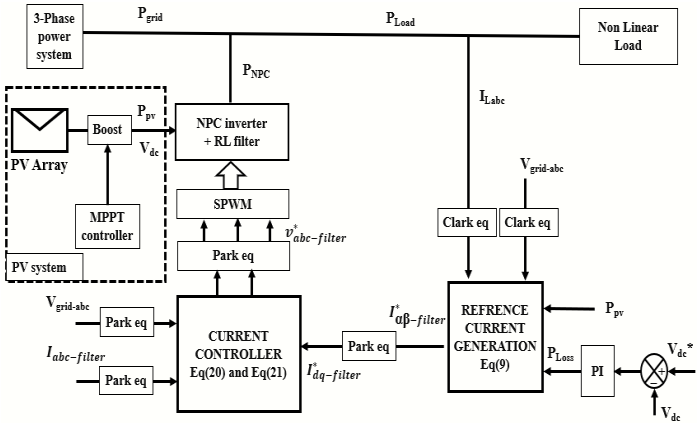

Figure 3. The block diagram of the control system

3.1. PQ theory of instantaneous real and active power

This control approach is employed to determine the reference currents for the control system with the aim of reducing the harmonic distortion coefficient [23]-[25]. To calculate the reference current values using the PQ theory, it is necessary to measure harmonic currents at the load side, grid voltage, as well as the loss component power from the dc-link voltage system control, in addition to the power generated by the PV panels. The PQ theory method involves transforming voltage and current variables from the a, b, c reference frame to the instantaneous signals of power, voltage, and current in the α−β reference frame [24].
There are the formulas for converting voltages and currents:

$$\begin{bmatrix} V_{\alpha-\mathrm{grid}} \\ V_{\beta-\mathrm{grid}} \end{bmatrix} = \sqrt{\frac{2}{3}} \begin{bmatrix} 1 & -\frac{1}{2} & -\frac{1}{2} \\ 0 & \frac{\sqrt{3}}{2} & -\frac{\sqrt{3}}{2} \end{bmatrix} \begin{bmatrix} V_{\mathrm{a-grid}} \\ V_{b-grid} \\ V_{\mathrm{c-grid}} \end{bmatrix} \quad (4)$$

$$\begin{bmatrix} i_{\alpha-\mathrm{Load}} \\ i_{\beta-\mathrm{Load}} \end{bmatrix} = \sqrt{\frac{2}{3}} \begin{bmatrix} 1 & -\frac{1}{2} & -\frac{1}{2} \\ 0 & \frac{\sqrt{3}}{2} & -\frac{\sqrt{3}}{2} \end{bmatrix} \begin{bmatrix} i_{\mathrm{a-Load}} \\ i_{b-\mathrm{Load}} \\ i_{\mathrm{c-Load}} \end{bmatrix} \quad (5)$$

The instantaneous active and reactive powers are calculated based on (6):

$$\begin{bmatrix} p \\ q \end{bmatrix} = \begin{bmatrix} V_{\alpha-\mathrm{grid}} & V_{\beta-\mathrm{grid}} \\ -V_{\beta-\mathrm{grid}} & V_{\alpha-\mathrm{grid}} \end{bmatrix} \begin{bmatrix} i_{\alpha-\mathrm{Load}} \\ i_{\beta-\mathrm{Load}} \end{bmatrix} \quad (6)$$

Where both instantaneous p and q have two components, one is direct component and the other is alternating component. Therefore, it is written as (7) and (8):

$$p = \bar{p} + \tilde{p} \quad (7)$$

$$q = \bar{q} + \tilde{q} \quad (8)$$

where $\bar{p}, \bar{q}$ are direct powers resulting from the active components of voltage and current and $\tilde{p}, \tilde{q}$ are alternating powers related to the harmonic currents and they are resulting from the alternating components of voltage and current.

The active and reactive alternating powers that cause harmonic currents are calculated by passing the power signal through a low-pass filter or a high-pass filter. In this research, the Low pass filter will be used to specify the frequency band to be compensated by the effective filter. In the last step, the reference currents in α, β frame will be calculated as (9):

$$\begin{bmatrix} \mathrm{i}_{\alpha-\mathrm{ref}} \\ \mathrm{i}_{\beta-\mathrm{ref}} \end{bmatrix} = \frac{1}{\mathrm{V}_{\alpha-\mathrm{grid}^2}+\mathrm{V}_{\beta-\mathrm{grid}^2}} \begin{bmatrix} \mathrm{V}_{\alpha-\mathrm{grid}} & \mathrm{V}_{\beta-\mathrm{grid}} \\ \mathrm{V}_{\beta-\mathrm{grid}} & -\mathrm{V}_{\alpha-\mathrm{grid}} \end{bmatrix} \begin{bmatrix} \widetilde{\mathrm{p_c}} \\ \bar{\mathrm{q}} \end{bmatrix} \quad (9)$$

where:

$$\widetilde{p_c} = p_{pv} + p - \bar{p} + p_{loss} \quad (10)$$

3.2. Design of current controllers

Lyapunov's theory will be used to design the current controller in the inner loop, but first it is necessary to know the dynamic equations relating to the filter's currents which are given as (11) and (12) [26]-[28]:

$$\mathrm{L_{filter}} \frac{\mathrm{di_{dfilter}}}{\mathrm{dt}} = \mathrm{V_d} - \mathrm{u_{dfilter}} + \omega_s \mathrm{L_{filter}} \mathrm{i_{qfilter}} - \mathrm{R_{filter}} \mathrm{i_{dfilter}} \quad (11)$$

$$L_{filter}\frac{di_{qfilter}}{dt} = V_q - u_{qfilter} - \omega_s L_{filter} i_{dfilter} - R_{filter} i_{qfilter} \quad (12)$$

Let's first assume:

$$e_d = i^*_{dfilter} - i_{dfilter} \quad (13)$$

After deriving the relation (13) and substituting the relation (11) it is obtained:

$$\dot{e}_d = \frac{di^*_{dfilter}}{dt} + \frac{R_{filter}}{L_{filter}} i_{dfilter} - \omega_s i_{qfilter} - \frac{V_d}{L_{filter}} + \frac{u_{dfilter}}{L_{filter}} \quad (14)$$

Suppose the formula for the Lyapunov function is:

$$v_d = 0.5\gamma_1 {e_d}^2 + 0.5\gamma_2 {z_d}^2 \quad (15)$$

Where:

$$z_d = \int e_d \, dt \quad (16)$$

After deriving the relation (15) and substituting the relation (16) it is obtained:

$$\dot{v_d} = \gamma_1 \dot{e}_d e_d + \gamma_2 z_d \dot{z_d} \quad (17)$$

After substituting the relation (14) it is obtained:

$$\dot{v_d} = \gamma_1 \left(\frac{di^*_{dfilter}}{dt} + \frac{R_{filter}}{L_{filter}} i_{dfilter} - \omega_s i_{qfilter} - \frac{V_d}{L_{filter}} + \frac{u_{dfilter}}{L_{filter}}\right) e_d + \gamma_2 z_d e_d \quad (18)$$

By fixing (18) it can be obtained:

$$\dot{v_d} = -k_1 {e_d}^2 + e_d\left(\gamma_1 \frac{di^*_{dfilter}}{dt} + \gamma_1 \frac{R_{filter}}{L_{filter}} i_{dfilter} - \gamma_1 \omega_s i_{qfilter} - \gamma_1 \frac{V_d}{L_{filter}} + \gamma_1 \frac{u_{dfilter}}{L_{filter}} + \gamma_2 z_d + k_1 e_d\right) \quad (19)$$

to make derivative of Lyapunov function (v_d) negative, it must be:

$$u^*_{dfilter} = \frac{L_{filter}}{\gamma_1}\left(-\gamma_1 \frac{di^*_{dfilter}}{dt} - \gamma_1 \frac{R_{filter}}{L_{filter}} i_{dfilter} + \gamma_1 \omega_s i_{qfilter} + \gamma_1 \frac{V_d}{L_{filter}} - \gamma_2 z_d - k_1 e_d\right) \quad (20)$$

In the same way, in order to regulate the current on the q axis, one can obtain:

$$u^*_{qfilter} = \frac{L_{filter}}{\gamma_3}\left(-\gamma_3 \frac{di^*_{qfilter}}{dt} - \gamma_3 \frac{R_{filter}}{L_{filter}} i_{qfilter} - \gamma_3 \omega_s i_{dfilter} + \gamma_3 \frac{V_q}{L_{filter}} - \gamma_4 z_q - k_2 e_q\right) \quad (21)$$

where:

$$e_q = i^*_{qfilter} - i_{qfilter} \quad (22)$$

$$z_q = \int e_q \, dt \quad (23)$$

γ_i, k_i are positive constants.

It should be noted that to move from abc frame to d,q frame, (24) is used, and to move from α, β frame to d,q frame, (25) is used.

$$\begin{bmatrix} X_d \\ X_q \end{bmatrix} = \sqrt{3/2} \begin{bmatrix} \cos(\theta) & \cos(\theta - \frac{2\pi}{3}) & \cos(\theta + \frac{2\pi}{3}) \\ -\sin(\theta) & -\sin(\theta - \frac{2\pi}{3}) & -\sin(\theta + \frac{2\pi}{3}) \end{bmatrix} \begin{bmatrix} X_a \\ X_b \\ X_c \end{bmatrix} \quad (24)$$

$$\begin{bmatrix} X_d \\ X_q \end{bmatrix} = \begin{bmatrix} \cos(\theta) & \sin(\theta) \\ -\sin(\theta) & \cos(\theta) \end{bmatrix} \begin{bmatrix} X_\alpha \\ X_\beta \end{bmatrix} \quad (25)$$

3.2. V_{dc} link controller

As has been mentioned previously, the power produced from the PV panels is transmitted through the dc-dc boost converter, which is controlled by the maximum power point tracking unit, which maintains the voltage value on the panels array terminals equal to the voltage corresponding to the maximum power point V_{mpp}, while the value of the output voltage of this converter (V_{dc}), which is called DC-link voltage is controlled by the inverter control system which is connected to the electric grid. This control system includes two control loops, in outer loop a PI controller is used to regulate the voltage V_{dc} at desired value, and the inner loop which used to regulate the currents exchanged with the grid. The parameters of the DC-link voltage controller (Kp and Ki) have been chosen empirically so as to obtain the best possible response.

4. SIMULATION RESULTS

Simulations were conducted for using the 3 level NPC inverter in the PV/grid interfacing system under varying load resistance values and different levels of solar radiation, where Figure 4 illustrates the variations in the resistance (Figure 4(a)) and the power (Figure 4(b)) of the nonlinear load, and Figure 5 shows the profile of solar radiation changes, which is at a value of 900 w/m^2 during the period 0-1.2 and at a value of 1000 w/m^2 during the period from 1.2-3 secs. The performance of the control system based on

integral back-stepping controller for current regulation and PI-controller for DC-link voltage regulation was initially tested. Table 2 contains the load and PV/grid parameters, and Table 3 contains the design parameters of the controllers.

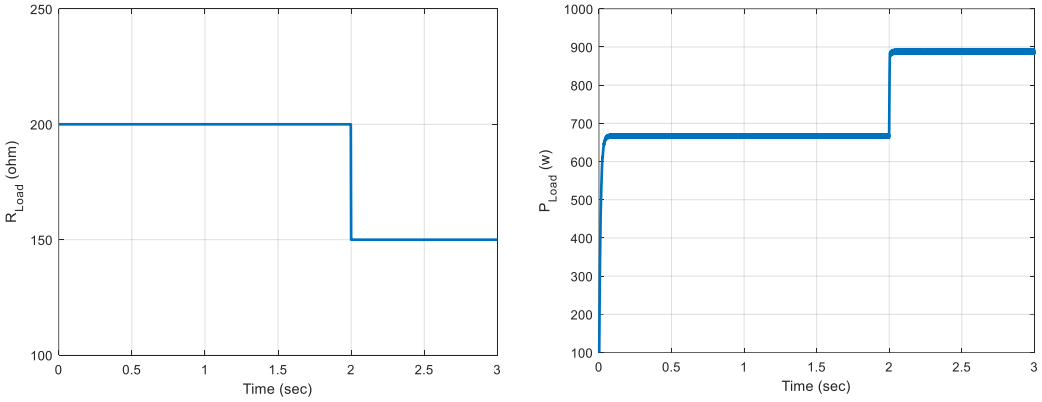

(a) (b)

Figure 4. Changes of; (a) resistance of the nonlinear load and (b) power of the nonlinear load

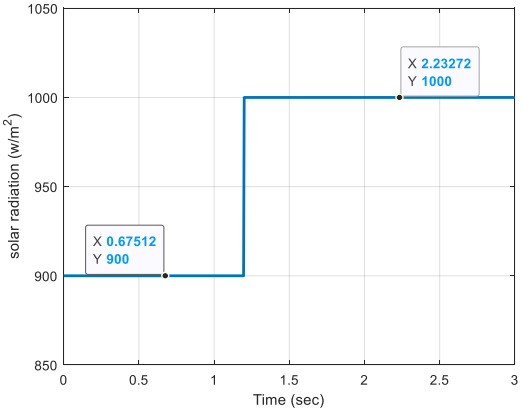

Figure 5. The profile of solar radiation changes

Table 2. PV/grid characteristics

System	Parameter	Value
NPC inverter	Level	3
	C_{NPC}	0.009 F
Decoupling filter	R_{filter}	0.5 Ω
	L_{filter}	6e-3 H
Nonlinear load	R_{Load}	200 Ω
	L_{Load}	10e-3 H
Power grid	V_g	220 v
	F_g	50 Hz

Table 3. Control system parameters

AC current back stepping controller		AC current PI controller		DC voltage PI controller	
γ_1	0.5	k_{pac}	50	k_p	400
γ_2	10e5				
γ_3	0.5				
γ_4	10e5	k_{iac}	250	k_i	2500
k_1	50e3				
k_2	50e3				

The Figure 6 shows the system response for dc link voltage regulation, where it can be seen that PI controller achieves good dynamic performance with a static error of zero despite the change in the value of

solar radiation or energy of load. The results of controlling the currents in the inner loop are illustrated by the Figures 7 and 8, where it is noted that the control system achieves a high dynamic, fast response and accuracy in tracking the reference signals calculated using relationship (9) which contributes to reducing the value of the total distortion factor to a value less than 5% as shown in Figures 9(a) and (b), while the value of the distortion factor caused by the non-linear load connected with the grid equal to 30.5%.

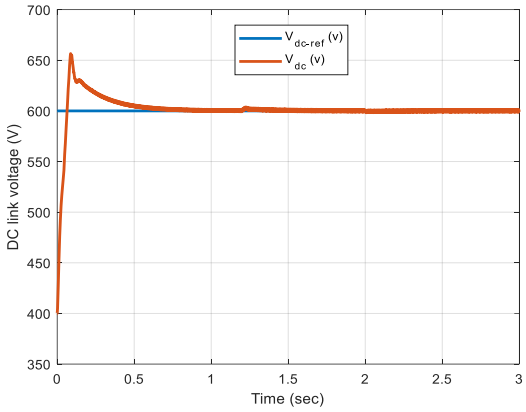

Figure 6. The system response for DC link voltage regulation

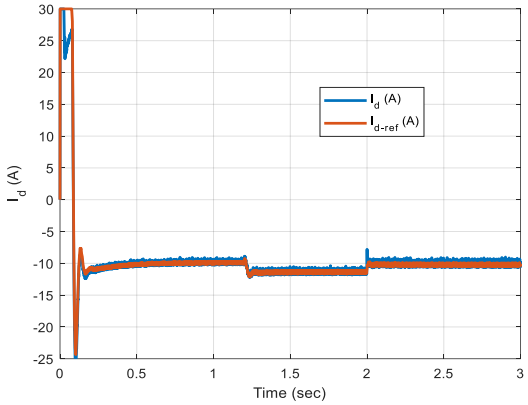

Figure 7. The system response for i_d regulation

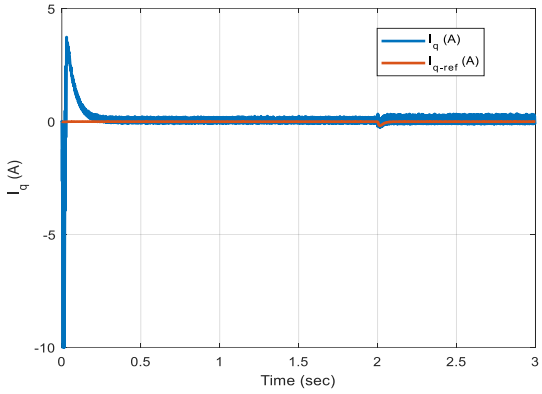

Figure 8. The system response for i_q regulation

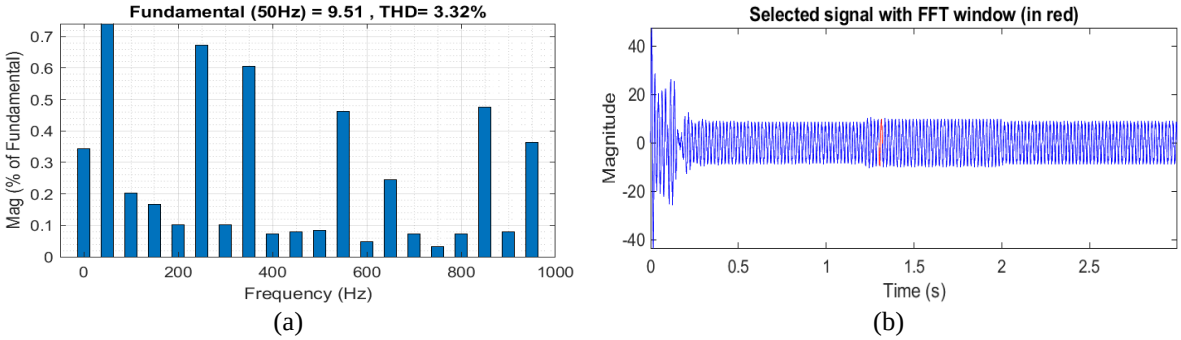

(a) (b)

Figure 9. FFT analyzer for the grid current; (a) the mag (%) and (b) the magnitude of the signal

With the increasing the value of solar radiation, the power provided by the solar electric generation system will increase, and this is shown in the Figure 10, as it is noted that the generated power at the output of the inverter is distributed between the load and the electrical grid. It is noted that the power transmitted through the voltage inverter (P_{npc}) feeds the load and the surplus goes towards the grid. The Figure 11 shows the voltage and current signals of the electrical grid, as it can be seen that they are in phase, meaning that the power factor is equal to one. Thus, it can be said that the PV generation system contributes to improving the quality of the electrical grid.

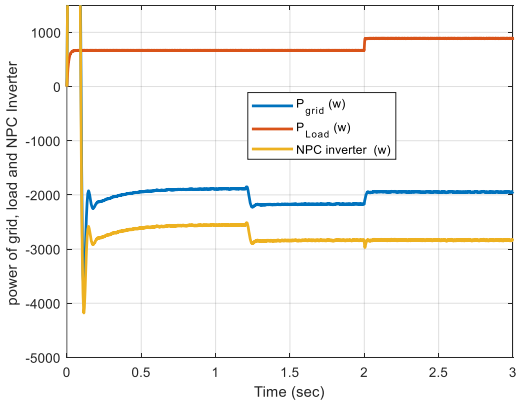

Figure 10. Flow of power through the electrical system

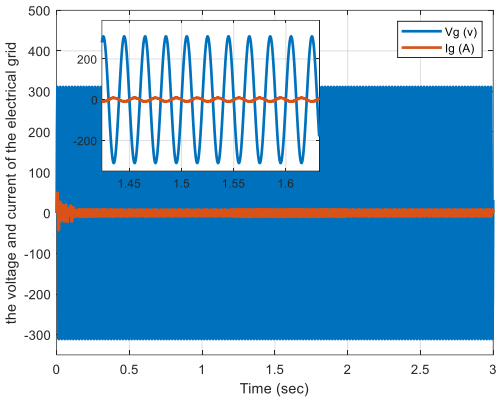

Figure 11. The voltage and current of the grid

The results of the comparison for THD value between using a conventional inverter and an NPC type inverter are reviewed with the applied of two different control techniques, namely the integral back stepping technique and PI controller. The Figure 12 show the total harmonic distortion factor changes for different approaches of controlling, where these results can be overlaid in the Table 4 it is noted that the performance of the system when using a three-level NPC inverter with regulating the currents according to the integral back stepping technique is the best compared to the rest of the cases, whether reduced level (RL) value equal to 200 Ω or 150 Ω. In second place comes the case of using the same inverter, but with regulated currents using PI controller, this illustrates the importance of using a three level NPC inverter in reducing the harmonic distortion factor and improving the quality of the electrical grid.

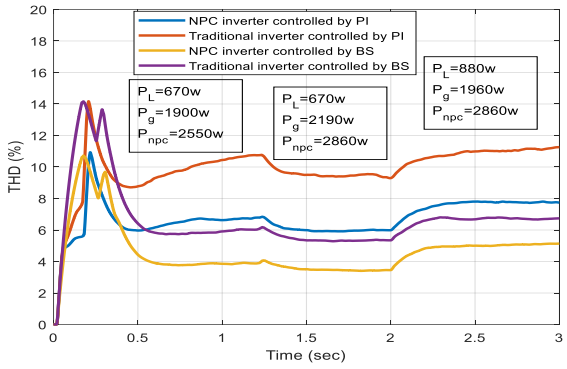

Figure 12. Total harmonic distortion factor changes for different control methods

Table 4. The simulation results

Inverter	THD when R_L=200 Ω (%)	THD when R_L=150 Ω (%)
3-level NPC inverter controlled by integral back-stepping controller	3.3	5
Three-level NPC inverter controlled by PI controller	5.3	6.7
Traditional inverter controlled by integral back-stepping controller	6	7.8
Traditional inverter controlled by PI controller	9.4	11

5. CONCLUSION

This study focuses on a comparison of two grid-connected converter topologies in a PV generation system connected to a three-phase grid feeding a non-linear load, as well as two control techniques for this converter and their impact on the total harmonic distortion coefficient value. The solar panels were connected to the grid in two steps. The first stage uses a P&O algorithm to track the maximum power point. The second stage uses a three-phase inverter to transfer ac power with the lowest total harmonic distortion coefficient. The simulation results were first presented for a three-level inverter controlled by the IBS technique, which demonstrated dynamic performance and a quick and accurate response to reference signals.

The simulation results are then presented for four scenarios: three-level inverter controlled using the IBS technique, three-level inverter controlled using PI controllers, conventional inverter controlled using the IBS technique, and conventional inverter controlled using PI controllers. It should be noted that PQ theory was used to determine the reference values for the currents in the inner loop in order to reduce the distortion harmonic factor, which was reduced to values ranging from 3.4-5% for a 3-level NPC inverter controlled using the IBS technique and to values ranging from 5.3-6.7% when the same inverter was controlled using a PI controller. THD values for traditional inverters range from 6-8% when controlled by the IBS technique to 9.4-11% when controlled by the PI controller.

REFERENCES

[1] M. Y. Worku and M. A. Abido, "Grid connected PV system using ANFIS based MPPT controller in real time," *Renewable Energy & Power Quality Journal*, pp. 35–40, May 2016, doi: 10.24084/repqj14.220.

[2] N. Debdouche, B. Deffaf, H. Benbouhenni, L. Zarour, and M. I. Mosaad, "Direct power control for Three-Level multifunctional voltage source inverter of PV systems using a simplified Super-Twisting algorithm," *Energies*, vol. 16, no. 10, p. 4103, May 2023, doi: 10.3390/en16104103.

[3] B. Bendib, F. Krim, H. Belmili, M. F. Almi, and S. Boulouma, "Advanced Fuzzy MPPT controller for a stand-alone PV system," *Energy Procedia*, vol. 50, pp. 383–392, Jan. 2014, doi: 10.1016/j.egypro.2014.06.046.

[4] Y. Atifi, A. Raihani, and M. Kissaoui, "Smart Grid Production Cost Optimization by Bellman Algorithm," *Communications in computer and information science*, 2022, pp. 225–234, doi: 10.1007/978-3-031-20490-6_18.

[5] Z. Cabrane, M. Ouassaid, and M. Maâroufi, "Analysis and evaluation of battery-supercapacitor hybrid energy storage system for photovoltaic installation," *International Journal of Hydrogen Energy*, vol. 41, no. 45, pp. 20897–20907, Dec. 2016, doi: 10.1016/j.ijhydene.2016.06.141.

[6] A. Sabo, B. Y. Kolapo, T. E. Odoh, M. Dyari, N. I. A. Wahab, and V. Veerasamy, "Solar, Wind and their hybridization Integration for Multi-Machine Power System Oscillation Controllers Optimization: A review," *Energies*, vol. 16, no. 1, p. 24, Dec. 2022, doi: 10.3390/en16010024.

[7] M. Et-taoussi and H. Ouadi, "Power quality control for grid connected Photovoltaic system with Neutral Point Converter," *2016 International Renewable and Sustainable Energy Conference (IRSEC)*, Marrakech, Morocco, 2016, pp. 1040-1045, doi: 10.1109/IRSEC.2016.7983887.

[8] J. P. Ram, H. Manghani, D. S. Pillai, T. N. Babu, M. Miyatake, and N. Rajasekar, "Analysis on solar PV emulators: A review," *Renewable & Sustainable Energy Reviews*, vol. 81, pp. 149–160, Jan. 2018, doi: 10.1016/j.rser.2017.07.039.

[9] R. Shah, N. Mithulananthan, R. C. Bansal, and V. K. Ramachandaramurthy, "A review of key power system stability challenges for large-scale PV integration," *Renewable & Sustainable Energy Reviews*, vol. 41, pp. 1423–1436, Jan. 2015, doi: 10.1016/j.rser.2014.09.027.

[10] Y. Atifi, A. Raihani, M. Kissaoui, M. Hajjaj, and A. Bouaaddi, "Towards a smart photovoltaic panel: Numerical and experimental StudY," in *Springer eBooks*, 2023, pp. 788–793. doi: 10.1007/978-3-031-26254-8_114.

[11] T. Hamdi, K. Elleuch, H. Abid, and A. Toumi, "MPPT of a PV panel based on fuzzy logic and sliding mode controller," *2022 IEEE 21st International Ccnference on Sciences and Techniques of Automatic Control and Computer Engineering (STA)*, Dec. 2022, pp. 584-588, doi: 10.1109/sta56120.2022.10019214.

[12] D. Remoaldo and I. S. Jesus, "Analysis of a traditional and a fuzzy logic enhanced perturb and observe algorithm for the MPPT of a photovoltaic system," *Algorithms*, vol. 14, no. 1, p. 24, Jan. 2021, doi: 10.3390/a14010024.

[13] M. A. Abo-Sennah, M. A. El-Dabah, and A. E.-B. Mansour, "Maximum power point tracking techniques for photovoltaic systems: a comparative study," *International Journal of Electrical and Computer Engineering (IJECE)*, vol. 11, no. 1, pp. 57- 73, Feb. 2021, doi: 10.11591/ijece.v11i1.pp57-73.

[14] T. Esram and P. L. Chapman, "Comparison of photovoltaic array maximum power point tracking techniques," *IEEE Transactions on Energy Conversion*, vol. 22, no. 2, pp. 439–449, Jun. 2007, doi: 10.1109/tec.2006.874230.

[15] Ming-Fa Tsai, Chung-Shi Tseng, Guo-Dong Hong, and Shih-Hua Lin, "A novel MPPT control design for PV modules using neural network compensator," *2012 IEEE International Symposium on Industrial Electronics*, Hangzhou, 2012, pp. 1742-1747, doi: 10.1109/ISIE.2012.6237354.

[16] K. Anil, N. D. Kaushika, B. Singh, and N. Agarwal, "Simulation model of ANN based maximum power point tracking controller for solar PV system," *Solar Energy Materials and Solar Cells*, vol. 95, no. 2, pp. 773–778, Feb. 2011, doi: 10.1016/j.solmat.2010.10.022.

[17] F. Sebaaly, H. Vahedi, H. Y. Kanaan, N. Moubayed, and K. Al-Haddad, "Design and implementation of Space Vector Modulation- Based Sliding Mode Control for Grid-Connected 3L-NPC inverter," *IEEE Transactions on Industrial Electronics*, vol. 63, no. 12, pp. 7854–7863, Dec. 2016, doi: 10.1109/tie.2016.2563381.

[18] A. S. Maklakov, A. A. Radionov, and V. R. Gasiyarov, "Power factor correction and minimization THD in industrial grid viaReversible medium voltage AC drives based on 3L-NPC AFE rectifiers," *IECON 2016 - 42nd Annual Conference of the IEEE Industrial Electronics Society*, Florence, Italy, 2016, pp. 2551-2556, doi: 10.1109/IECON.2016.7793315.

[19] Z. J. Andaloussi, A. Raihani, A. E. Magri, R. Lajouad, and A. E. Fadili, "Novel nonlinear control and optimization strategies for hybrid renewable energy conversion system," *Modelling and Simulation in Engineering*, vol. 2021, pp. 1–20, Oct. 2021, doi: 10.1155/2021/3519490.

[20] M. Novak, T. Dragicevic, and F. Blaabjerg, "Weighting factor design based on Artificial Neural Network for Finite Set MPC operated 3L-NPC converter," *2019 IEEE Applied Power Electronics Conference and Exposition (APEC)*, Anaheim, CA, USA, 2019, pp. 77-82, doi: 10.1109/APEC.2019.8722062.

[21] R. Sen, A. Garg, and A. Singh, "Modeling of PV array using P&O algorithm in boost converter," *2017 International Conference on Computing and Communication Technologies for Smart Nation (IC3TSN)*, Gurgaon, India, 2017, pp. 231-236, doi: 10.1109/IC3TSN.2017.8284482.

[22] J. Khanam and F. Sy, "Modeling of a photovoltaic array in MATLA.B Simulink and maximum power point tracking using neural network," *Journal of Electrical & Electronic Systems*, vol. 07, no. 03, pp. 40-46, Jan. 2018, doi: 10.4172/2332-0796.1000263.

[23] S. S. Dheeban and N. B. M. Selvan, "ANFIS-based power quality improvement by Photovoltaic Integrated UPQC at distribution system," *Iete Journal of Research*, vol. 69, no. 5, pp. 2353–2371, Feb. 2021, doi: 10.1080/03772063.2021.1888325.

[24] A. A. Imam, R. Kumar, and Y. Al-Turki, "Modeling and simulation of a PI controlled shunt active power filter for power quality enhancement based on P-Q theory," *Electronics*, vol. 9, no. 4, p. 637, Apr. 2020, doi: 10.3390/electronics9040637.

[25] B. V. Siva, B. M. Babu, L. R. Srinivas, and S. S. Tulasiram, "Design of Shunt Active Power Filter for Improvement of Power Quality with Artificial Intelligence Techniques," *International Journal of Advanced Research in Electrical, Electronics and Instrumentation Energy*, vol. 03, no. 08, pp. 11304–11314, Aug. 2014, doi: 10.15662/ijareeie.2014.0308053.

[26] F.-E. Tahiri, K. Chikh, M. Khafallah, and A. E. Afia, "Design and implementation of different control strategies of unit Power Factor Three-Phase PWM rectifier for output voltage regulation," *Advances in Science, Technology & Innovation*, pp. 29-38, 2019, doi: 10.1007/978-3-030-05276-8_4.

[27] X. Zhou, J. Wang, and Y. Ma, "Linear active disturbance rejection control of Grid-Connected photovoltaic inverter based on deviation control principle," *Energies*, vol. 13, no. 15, p. 3790, Jul. 2020, doi: 10.3390/en13153790.

[28] M. M. Gulzar, A. Iqbal, D. Sibtain, and M. Khalid, "An Innovative Converterless Solar PV Control Strategy for a Grid Connected Hybrid PV/Wind/Fuel-Cell System Coupled With Battery Energy Storage," in *IEEE Access*, vol. 11, pp. 23245-23259, 2023, doi: 10.1109/ACCESS.2023.3252891.

BIOGRAPHIES OF AUTHORS

Youness Atifi is a Ph.D. student at Hassan II University in Casablanca, affiliated with the Electrical Engineering and Intelligent Systems Laboratory (EEIS) at ENSET Mohammedia. He obtained his electrical engineering aggregation diploma in 2021. Currently, he's an electrical engineering professor at preparatory classes for higher technician diploma. His research interests include optimization, observation and nonlinear control of AC machines, and renewable energy. He can be contacted at email: atifi.youness@gmail.com.

Abdelhadi Raihani was appointed as a professor in Electronics Engineering at Hassan II University of Casablanca, ENSET Institute, Mohammedia Morocco since 1991. He received the B.S. degree in Applied Electronics in 1991 from the ENSET Institute. He has his DEA diploma in Information Processing from Ben M'sik University of Casablanca in 1994. He received the Ph.D. in Parallel Architectures Application and Image Processing from the Ain Chock University of Casablanca in 1998. He currently serves as a full Professor in the Department of Electrical Engineering at ENSET of Mohammedia. His research topics are various and large in multiple domains of medical image processing and electrical engineering, energy management systems, power, and energy systems control and smart grids. He has published over than 74 papers in distinguished scientific journals and more than 60 papers in international conferences. He supervised and delivered more than 15 PhD theses. He worked closely in national research programs with IRESEN under the grant "Green INNO Project/UPISREE". He can be contacted at email: raihani@enset-media.ac.ma.

Mohammed Kissaoui was born in 1974. He received the Aggregation of Electrical Engineering from the ENSET, Rabat, Morocco, in 2006, the Ph.D. degree in control engineering from the Université de Mohammed V, Rabat, Morocco, in 2018, under the supervision of Prof. F. Giri and Prof. F. Z. Chaoui. Currently, he is Professor at the Ecole Normale Supérieure d'Enseignement Technique (ENSET), Hassan II university, Mohammedia, Morocco. His research interests include optimization, observation and nonlinear control of uninterruptible power supplies, active power filters, and AC machines. He has coauthored several papers on these topics. He can be contacted at email: kissaouimed@gmail.com.

Rachid Lajouad was born in 1974. He received Ph.D. degree in electrical engineering from Mohammed V University, Rabat, Morocco, in 2016. Currently, he is a professor at the Hassan II University, Casablanca, Morocco. His research interests include optimization, observation and nonlinear control of AC machines, and renewable energy. He has published several journal/conference papers on these topics. He can be contacted at email: dsa.lajouad@gmail.com.

Khalid Errakkas is a dedicated and experienced high school teacher specializing in electrical engineering since 2016. He obtained his master's degree in Electronics and Embedded Systems from the Faculty of Sciences and Techniques, Errachidia, at Moulay Ismail University in 2020. In 2023, he embarked on his doctoral journey in Engineering Sciences at Ecole Normal Superior of Technical Education (ENSET) Mohammedia, Hassan II University, Casablanca, with a focus on energy management and optimization methods for the microgrids within the Electrical Engineering and Intelligent Systems Laboratory. He can be contacted at email: khalid.errakkas@gmail.com.